

Shape Evolution of SrTiO₃ Crystals During Coarsening in a Titania-Rich Liquid

Tomoko Sano,* Chang-Soo Kim,* and Gregory S. Rohrer†,*

Department of Materials Science and Engineering, Carnegie Mellon University, Pittsburgh, Pennsylvania 15213-3890

To identify factors that might affect capillary driving forces and interface structure-dependent mechanisms for coarsening, we have used a stereological analysis to determine the changes in the morphology of SrTiO₃ crystals in contact with a titania-rich liquid at 1500°C. A combination of flat and curved surfaces is observed in contact with the liquid. The {100} surface is the most common, followed by {110}. A range of surfaces in the <100> zone are also found, but with a lower frequency. The areas of the {100} and {110} surfaces are approximately equal at the initial stage, but after 24 h of growth, the {100} surface area is more than twice as great as the {110} surface area. At this point, {100} surfaces make up more than 25% of the surface area in contact with the liquid. The results suggest that morphological changes during growth continuously reduce the average surface energy and interface mobility. This provides a plausible explanation for coarsening rates that decrease faster than predicted by the classical theory.

I. Introduction

IN the classical coarsening theory, the average crystal size $\langle r \rangle$ increases with time:

$$\langle r \rangle - \langle r_0 \rangle = (Kt)^n \quad (1)$$

where K is a positive constant, $\langle r_0 \rangle$ is the initial average radius, and n is a constant less than or equal to 1/2 that depends on the rate-limiting step of the process.^{1,2} Although the original derivation of this law assumes isotropic interface energies, Mullins³ has shown that as long as the crystal size distributions maintain statistical self-similarity and the interface energy is differentiable at all orientations, then the anisotropy of the interface energy does not alter the kinetics described by Eq. (1). While the condition on the form of the energy anisotropy might not be met for most ceramics, simulations using energy functions with singularities have demonstrated that classical kinetics are preserved.^{4,5} However, classical kinetics are not always observed in the coarsening of ceramics. For example, coarsening has been used to grow single crystals of ceramics by annealing a seed crystal in contact with a polycrystalline material combined with a lower melting intergranular liquid; the most well-documented case is that of Pb(Mg_{1/3}Nb_{2/3})O_{3-x}·PbTiO₃.^{6–10} The published data suggest that there is a continuous reduction in the growth rate beyond that predicted by Eq. (1), as if the growth constant, K , is decreasing with time.^{8–10} This phenomenon will be referred to here as non-classical coarsening kinetics.

One possible explanation for the non-classical kinetics is the development of porosity, which increasingly retards interface

motion as growth proceeds. However, recent work indicates that the growth rate reduction does not completely disappear when porosity is eliminated.¹¹ Another possible explanation for the non-classical kinetics is that the crystals undergo continuous morphological changes as they grow so that the fraction of slow moving or low energy surfaces in contact with the liquid continuously increases, reducing the growth rate faster than predicted by Eq. (1). For example, if the starting materials are milled, then the particles will have roughly equiaxed shapes at the start of coarsening. When annealed, growing crystals will adopt shapes that reflect the relative growth (or dissolution) rates of the different orientations. As coarsening progresses, we expect that slow-growing faces will cover more of the surface and fast-growing faces will disappear. If the slow-growing surfaces are also low-energy surfaces, then the overall driving force will be reduced by volume-conserving shape changes, even in the absence of growth. Also, if the slow-growing faces are singular, then growth and shrinkage may be limited by the surface attachment/detachment rate, the motion of ledges, or the nucleation of new layers.^{12–14}

The problem of how crystal shape, interface structure, and coarsening rate are related had been addressed in a number of recent theoretical^{4,5,12–14} and experimental^{15–21} papers. The experimental approach has been qualitative, using micrographs to demonstrate that interfaces are rough or flat and, in the latter case, that certain orientations are preferred over others.^{15–21} The theoretical papers, on the other hand, make quantitative predictions about size and shape distributions.^{4,5,12,13} To test the validity of these models, there is a clear need to provide quantitative data on the average crystal shape, the fractional area of singular surfaces, and how these quantities change during coarsening. To address this problem, we have developed a stereological procedure for measuring average crystal habits from planar sections.^{22,23} Previously, this procedure has been used to measure the distribution of bounding WC interfaces in Co, but only at a single point in time.²⁴ In the current paper, a new procedure is used to quantitatively determine how the crystallographic distribution of bounding surfaces changes as an anisotropic phase coarsens. The objective of the paper is to demonstrate that continuous morphological changes do occur during coarsening and that these changes provide a plausible mechanism for non-classical coarsening kinetics. This should be a general phenomenon, and occur in any anisotropic system. As a model, we study the coarsening of SrTiO₃ in a titania-rich liquid at 1500°C. This system is not expected to have the time-dependent composition variations that are expected to influence the morphological evolution of Pb(Mg_{1/3}Nb_{2/3})O_{3-x}·PbTiO₃.¹⁰

II. Experimental Procedure

The SrTiO₃–TiO₂ samples were formulated so that at the annealing temperature of 1500°C, they would consist of a two-phase mixture with 85% volume fraction solid SrTiO₃ and 15% volume fraction of a titania-rich liquid. The liquid comprised of 33.3 mol% SrTiO₃ and 66.7 mol% TiO₂.²⁵ SrTiO₃ and TiO₂ powders (99% pure) were mixed and then milled with ethanol and 1 cm glass balls for 5 h. Inspection of the powders at this

D. J. Green—contributing editor

Manuscript No. 10952. Received March 30, 2004; approved September 16, 2004. Supported primarily by the MRSEC program of the National Science Foundation under Award Number DMR-0079996 and partially by NASA under grant number 8-1674. *Member, American Ceramic Society. †Author to whom correspondence should be addressed. e-mail: gr20@andrew.cmu.edu

point by scanning electron microscopy showed agglomerates of submicron particles with no obvious flat surfaces or consistent shapes. After drying, the powder was mixed with a small amount of polyethylene glycol binder and deionized water, and then uniaxially pressed to 1700 psi. The consolidated samples were then degassed in vacuum at 800°C for 25 h before annealing in air at 1500°C. The samples were ramped to 1500°C at a rate of 5°C/min and then held at this temperature for times ranging from 0 to 24 h. The samples were then lapped with a 3 μm alumina slurry and polished with a 0.02 μm colloidal silica slurry.

The shapes of the SrTiO₃ crystals intersecting the section plane were determined from atomic force microscope (AFM) images. The AFM (Park Scientific Instruments, Sunnyvale, CA) was operated in contact mode, recording images with a resolution of 512 \times 512 pixels. Crystal orientation maps on planar sections were obtained using an electron-backscattered diffraction (EBSD) mapping system (EDAX/TSL, Draper, UT) integrated with a scanning electron microscope (Model XL40 FEG, Phillips, Eindhoven, the Netherlands). Orientation maps were recorded at a 60° tilt with a 20 kV beam. The step sizes for the orientation mapping were 0.3 and 1.6 μm for the 0 and 24 h sample, respectively.

The objective was to determine the distributions of SrTiO₃ crystals surfaces, $\lambda(\mathbf{n})$, where \mathbf{n} is the interface normal in the crystal reference frame and λ is the relative area, measured in multiples of a random distribution (MRD). For an isotropic distribution of interfaces, λ is unity for all \mathbf{n} . In the anisotropic case, values of λ above or below unity indicate relative areas larger or smaller than expected in the isotropic case. Stereological procedures for measuring the interface distribution have already been described for the case where there are a small number of flat facets²² and where there is a continuous distribution of surfaces.²³ Here, we use the latter procedure, since the samples exhibit both flat and curved interfaces. The method works on the principle that knowledge of the crystal orientation and the direction along which an interface intersects the plane of observation allows a finite set of possible orientations of the interface plane to be specified. By making many observations of similar crystals in different orientations, the true interface orientations will occur in the set of possible orientations more frequently than any other.

The data needed for this analysis were obtained using a computer program to digitize the solid-liquid interface traces in AFM images. The interface traces were then correlated with the orientation data, as described previously.²⁴ Data sets for each sample contained 2800–3500 individual traces from more than 600 different crystal sections.

III. Results

Figure 1 shows AFM images of polished surfaces. The solidified eutectic phase (referred to henceforth as the liquid) appears with

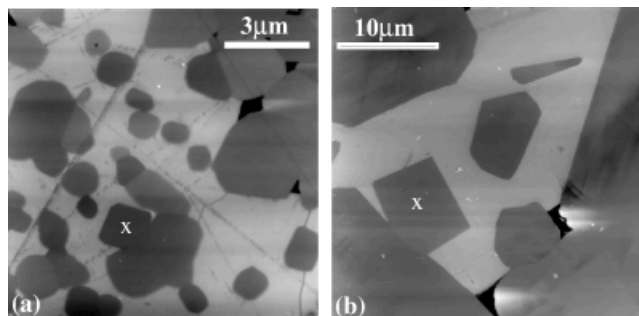


Fig. 1. Atomic force microscope images of SrTiO₃ embedded in a titania-rich matrix that was liquid at the coarsening temperature. (a) An example of the material after the 0 h anneal. (b) An example after the 24 h anneal. Note the change in scale. The crystals marked by the white “x” are oriented so that [100] is approximately parallel to the viewing direction.

a lighter contrast in these images because it polishes at a slower rate and is topographically higher than the SrTiO₃ crystals. While the interfaces between the SrTiO₃ and the liquid are easily identified on these planar sections, it should also be realized that the SrTiO₃ crystals impinge upon each other and form a three-dimensional skeletal network. From these typical images, it is clear that the growth shape of SrTiO₃ in liquid contains both curved surfaces and flat surfaces. For the 0 h sample, the average size of the grains used to measure $\lambda(\mathbf{n})$ was 0.8 μm and for the 24 h sample, the average size was 16 μm . This is noted only to recognize that larger grains were used in the later analysis; these figures were determined in limited fields of view and are not representative of the full distribution, which was generally not unimodal.

The distribution of surfaces, $\lambda(\mathbf{n})$, in the samples annealed for 0 and 24 h are shown in Fig. 2. All of the samples showed a relatively high population of {100}-type surfaces and a relatively low population of {111} surfaces. There is also a preference for planes in the $\langle 100 \rangle$ zones. At the earliest times, there are also peaks at the {110} positions, but they shrink with time and eventually disappear. Data extracted at intermediate times, but not shown here, are consistent with the trend that as the SrTiO₃ crystals are annealed for longer times, a larger fraction of the surface is bounded by {100}-type interfaces. The tendency for crystals to be bounded by {100} surfaces is confirmed by the shapes of the crystals in Fig. 1, which show examples of crystals that happen to be aligned so that [100] is nearly perpendicular to the sample plane. These grains are marked by an “x.” In these cases, the crystals display several straight edges oriented along $\langle 100 \rangle$ and separated by $\sim 90^\circ$. The distribution in Fig. 2(b) indicates that after 24 h, at least 1/4 of all the SrTiO₃ in contact with the liquid has the {100} orientation.

IV. Discussion

The distributions of SrTiO₃ surfaces shown in Fig. 2 are averages over the microstructure and result from the average of crystals that are both growing and shrinking. However, since the observations are weighted by area, the larger, growing crystals exert a greater influence on the distribution. Furthermore, many of the interface orientations are influenced by impingement with other grains. Therefore, it would be incorrect to interpret the distributions as accurate representations of the growth or equilibrium forms of SrTiO₃ under these conditions. What the results do provide is a statistical representation of the distribution of orientations in contact with the liquid. These are the surfaces that are receding or advancing as a result of the coarsening process and the changes in the area of these surfaces represent the driving force for coarsening.

The preference for surfaces with the {100} orientation is not surprising, considering recent measurements of the surface energy anisotropy of SrTiO₃ in air at 1400°C and the distribution of grain boundary planes at 1650°C.^{26,27} In air, the (100) orientation represents a minimum in the energy and grain boundaries showed a tendency to form on planes with the {100} orientation. According to the surface observations, orientations vicinal to {100} are also part of the equilibrium crystal shape. In other words, the six {100} facets on the roughly cubic equilibrium crystal shape are surrounded by smoothly curved surfaces. The current data show that surfaces in contact with the titania-rich liquid have many of the characteristics of the equilibrium crystal shape, including the curved regions around {100}.

The changes in the interface distribution reported here can potentially influence the kinetics of coarsening in several ways. First, we assume that the increase in the area of the {100} surfaces in contact with the fluid occurs because this is the slowest moving interface. As the crystal grows faster in other directions, the higher mobility interfaces disappear and leave behind the slowest interface. Since the {111} and neighboring orientations have negligible areas even at the earliest times, we conclude that these surfaces have mobilities that are significantly greater than those in

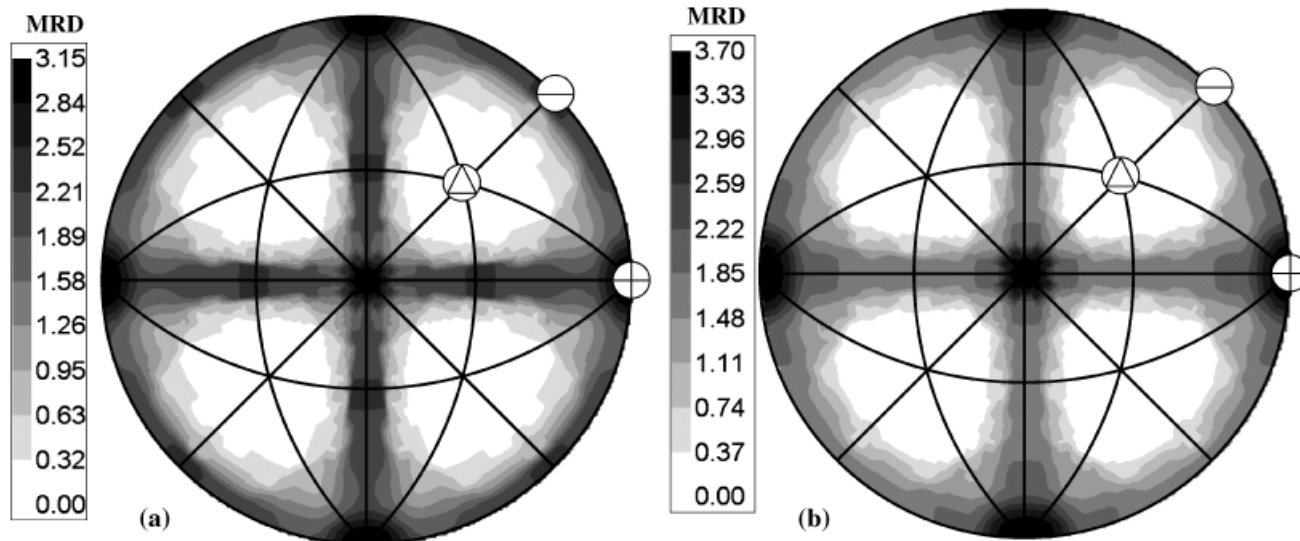


Fig. 2. The distribution of crystal surfaces, $\lambda(\mathbf{n})$, after (a) 0 h and (b) 24 h at 1500°C. The data are plotted in stereographic projection along [001] and the (100), (110), and (111) poles are marked with a circled “+,” “-,” and triangle, respectively.

the $\langle 100 \rangle$ zone and that the $\{100\}$ surfaces have the minimum mobility. Previous observations of macroscopic SrTiO₃ crystals growing into a matrix of fine grains indirectly suggest that the $\{110\}$ orientation grows more slowly than $\{100\}$.²⁸ Although the origin of this inconsistency is not clear, it should be noted that several aspects of the prior work differ from the present circumstances, such as the amount and composition of the liquid, and the defect structure and composition of the growing crystal. In any case, it can be concluded that as more of the total interfacial area is made up of the more slowly moving surfaces, the average growth rate will be diminished. The second factor that affects the coarsening rate is the change in the average surface energy. If the $\{100\}$ orientation has the minimum energy, then the driving force for growth is diminished as this orientation makes up a greater fraction of the total interfacial area.

Based on the observed changes in the interface distribution as a function of time; we proposed that morphological changes that result in crystals bounded by a higher fraction of low energy and slow-moving surfaces are a plausible explanation for non-classical coarsening rates. To determine whether or not this effect can retard growth to the extent observed in experiments,^{8–10} we will require more detailed information about the changes in the microstructure as a function of time. We are currently collecting detailed statistics on the evolution of the grain size distributions in these microstructures so that both size and shape changes can be quantitatively compared with models for coarsening in anisotropic materials.^{4,5,12,13}

V. Conclusion

When SrTiO₃ coarsens in a titania-rich liquid at 1500°C, the crystals change shape. As the initially equiaxed submicron crystals grow, they adopt cuboidal shapes for which the majority of the bounding interfaces consist of surfaces with $\{100\}$ orientations and surfaces in the $\langle 100 \rangle$ zone. The evolution of the shape during coarsening suggests that the $\{100\}$ surface has the lowest mobility and that slowly moving, low-energy surfaces become an increasing portion of the population as coarsening proceeds. These morphological changes provide a plausible explanation for non-classical coarsening kinetics that are observed in some anisotropic materials.

Acknowledgments

The authors thank E. P. Gorzkowski and M. P. Harmer for communicating the results of their work prior to publication.

References

- I. M. Lifshitz and V. V. Slyozov, “The Kinetics of Precipitation from Supersaturated Solid Solutions,” *J. Phys. Chem. Solids*, **19** [1/2] 35–50 (1961).
- C. Wagner, “Theory of Precipitate Aging via Dissolution/Reprecipitation; Ostwald Ripening,” *Z. Electrochem.*, **65** [7/8] 581–91 (1961).
- W. W. Mullins, “The Statistical Self Similarity Hypothesis in Grain Growth and Particle Coarsening,” *J. Appl. Phys.*, **59** [4] 1341–9 (1986).
- A. D. Rutenberg and B. P. Vollmayr-Lee, “Anisotropic Coarsening: Grain Shapes and Nonuniversal Persistence,” *Phys. Rev. Lett.*, **83** [19] 3772–75 (1999).
- E. Brosh and R. Z. Shneck, “Anisotropic Coarsening: The Effect of Interfacial Properties on the Shape of Grains,” *Modelling Simul. Mater. Sci. Eng.*, **8** [6] 815–23 (2000).
- A. Khan, F. A. Meschke, T. Li, A. M. Scotch, H. M. Chan, and M. P. Harmer, “Growth of Pb(Mg_{1/3}Nb_{2/3})O₃-35 mol% PbTiO₃ Single Crystals from (111) Substrates by Seeded Polycrystal Conversion,” *J. Am. Ceram. Soc.*, **82** [11] 2958–62 (1999).
- E. M. Sabolsky, G. L. Messing, and S. Trolier-McKinstry, “Kinetics of Templated Grain Growth of 0.65 Pb(Mg_{1/3}Nb_{2/3})O₃-0.35PbTiO₃,” *J. Am. Ceram. Soc.*, **84** [11] 2507–13 (2001).
- J. S. Wallace, J.-M. Huh, J. E. Blendell, and C. A. Handwerker, “Grain Growth and Twin Formation in 0.74PMN-0.26PT,” *J. Am. Ceram. Soc.*, **85** [6] 1581–4 (2002).
- A. Khan, E. P. Gorzkowski, A. M. Scotch, E. R. Leite, H. M. Chan, and M. P. Harmer, “Influence of Excess PbO Additions on $\{111\}$ Single Crystal Growth of Pb(Mg_{1/3}Nb_{2/3})O₃-35 mol% PbTiO₃ by Seeded Polycrystal Conversion,” *J. Am. Ceram. Soc.*, **86** [12] 2176–81 (2003).
- E. P. Gorzkowski, M. Watanabe, H. M. Chan, and M. P. Harmer, “Effect of Liquid Phase Chemistry on Single Crystal Growth in PMN-35PT,” *J. Am. Ceram. Soc.*, (in press).
- E. P. Gorzkowski, H. M. Chan, and M. P. Harmer, “Effect of PbO on the Kinetics of $\{001\}$ Pb(Mg_{1/3}Nb_{2/3})O₃-35mol% PbTiO₃ Single Crystals Grown into Fully Dense Matrices,” *J. Am. Ceram. Soc.*, submitted 2004.
- G. J. Shiflett, H. I. Aaronson, and T. H. Courtney, “Kinetics of Coarsening by the Ledge Mechanism,” *Acta Metall.*, **27** [3] 377–85 (1979).
- B. W. Sheldon and J. Rankin, “Step-Energy Barriers and Particle Shape Changes During Coarsening,” *J. Am. Ceram. Soc.*, **85** [3] 683–90 (2002).
- G. S. Rohrer, C. L. Rohrer, and W. W. Mullins, “Coarsening of Faceted Crystals,” *J. Am. Ceram. Soc.*, **85** [3] 675–82 (2002).
- S.-K. Kwon, S.-H. Hong, D.-Y. Kim, and N.-M. Hwang, “Coarsening Behavior of Tricalcium Silicate (C₃S) and Dicalcium Silicate (C₂S) Grains Dispersed in Clinker Melt,” *J. Am. Ceram. Soc.*, **83** [5] 1247–52 (2000).
- K.-S. Oh, J.-Y. Jun, D.-Y. Kim, and N.-M. Hwang, “Shape Dependence of the Coarsening Behavior of Niobium Carbide Grains Dispersed in a Liquid Iron Matrix,” *J. Am. Ceram. Soc.*, **83** [12] 3117–20 (2000).
- Y. K. Cho, S.-K. L. Kang, and D. Y. Yoon, “Dependence of Grain Growth and Grain-Boundary Structure on the Ba/Ti Ratio in BaTiO₃,” *J. Am. Ceram. Soc.*, **87** [1] 119–24 (2004).
- Y. K. Cho and D. Y. Yoon, “Faceting of High Angle Grain Boundaries in Ti-Excess BaTiO₃,” *J. Am. Ceram. Soc.*, **87** [3] 438–42 (2004).
- Y. K. Cho and D. Y. Yoon, “Surface Roughening Transition and Coarsening of NbC Grains in Liquid Cobalt-Rich Matrix,” *J. Am. Ceram. Soc.*, **87** [3] 443–8 (2004).
- M. J. Kim, Y. K. Cho, and D. Y. Yoon, “Facet-Defacet Transition of Grain Boundaries in Alumina,” *J. Am. Ceram. Soc.*, **87** [3] 455–9 (2004).

²¹M. J. Kim, Y. K. Cho, and D. Y. Yoon, "Singular Grain Boundaries in Alumina Doped with Silica," *J. Am. Ceram. Soc.*, **87** [3] 507–9 (2004).

²²D. M. Saylor and G. S. Rohrer, "Determining Crystal Habits from Observations of Planar Sections," *J. Amer. Ceram. Soc.*, **85** [11] 2799–804 (2002).

²³D. M. Saylor, B. S. El Dasher, B. L. Adams, and G. S. Rohrer, "Measuring the Five Parameter Grain Boundary Distribution From Observations of Planar Sections," *Metall. Mater. Trans.*, **35A** [8] 1981–9 (2004).

²⁴C.-S. Kim and G. S. Rohrer, "Geometric and Crystallographic Characterization of WC Surfaces and Grain Boundaries in WC–Co Composites," *Interface Sci.*, **12** [1] 19–27 (2004).

²⁵E. M. Levin, C. R. Robbins, and H. F. McMurdie, in *Phase Diagrams for Ceramists 1969 Supplement*, Edited by M. K. Reser. American Ceramic Society, Columbus, OH, 1969 (Figure 2334).

²⁶T. Sano, D. M. Saylor, and G. S. Rohrer, "Surface Energy Anisotropy of SrTiO₃ at 1400°C in Air," *J. Am. Ceram. Soc.*, **86** [11] 1933–9 (2003).

²⁷D. M. Saylor, B. S. El-Dasher, T. Sano, and G. S. Rohrer, "Distribution of Grain Boundaries in SrTiO₃ as a Function of Five Macroscopic Parameters," *J. Am. Ceram. Soc.*, **87** [4] 670–6 (2004).

²⁸S.-Y. Chung and S.-J. L. Kang, "Intergranular Amorphous Films and Dislocation Promoted Grain Growth in SrTiO₃," *Acta Mater.*, **51** [8] 2345–54 (2003). □